Impact of ionosphere on GPS-based precise orbit determination of Low Earth Orbiters

D. Arnold[1], Ch. Dahle[1], A. Jäggi[1], G. Beutler[1], U. Meyer[1], S. Schaer[1,2]

[1]Astronomical Institute, University of Bern, Bern, Switzerland
[2]Swiss Federal Office of Topography (swisstopo), Wabern, Switzerland

AGU G31B-1115
American Geophysical Union
Fall Meeting 2015
14-18 December 2015, San Francisco, USA

Introduction

Deficiencies in gravity fields derived from the orbital trajectories of Low Earth Orbiting (LEO) satellites determined by GPS-based Precise Orbit Determination (POD) were identified in recent years. The precise orbits of the Gravity Field and Steady-State Ocean Circulation Explorer (GOCE) mission are, e.g., severely affected by an increased position noise level over the geomagnetic poles and spurious signatures along the Earth's geomagnetic equator. This is illustrated in Figure 1, showing the carrier phase residuals of a reduced-dynamic orbit determination for GOCE in m, binned to the ionospheric piercing points at 450 km altitude (Jäggi et al., 2015a). The degradation of the orbits directly maps into the gravity fields recovered from these orbits.

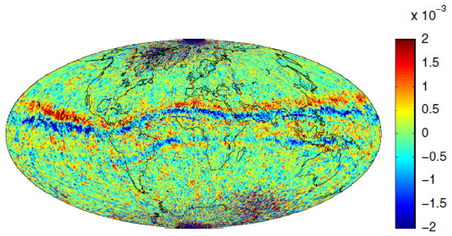

Figure 1: Carrier phase residuals of reduced-dynamic GOCE POD (in m). Systematic signatures along the geomagnetic equator are visible.

The same problems are evident, as well, for the on-going ESA missions Swarm and Sentinel. They are related to a disturbed GPS signal propagation through the Earth's ionosphere and indicate that the GPS observation model and/or the data pre-processing need to be improved. Furthermore, receiver-specific tracking problems under difficult ionospheric conditions might play an important role.

GPS and Ionosphere

The propagation of a microwave signal of frequency f emitted by GPS satellites is dispersively affected by the free electrons in the Earth's ionosphere:

$$\Delta\rho_{\text{ion}} = \pm\frac{C_X}{2} E f^{-2} + \mathcal{O}(f^{-3}) \,, \qquad (1)$$

where $\Delta\rho_{\text{ion}}$ is the path delay due to the ionosphere, $C_X/2 \approx 40\,\text{m}^3\text{s}^{-2}$ and $E = \int N_e(\rho) d\rho$ is the line-of-sight total electron content (TEC), obtained by integrating the electron density N_e along the ray path. The negative sign in Eq. (1) refers to the phase advance (phase observations), the positive sign to the group delay (code observations), respectively. The terms $\mathcal{O}(f^{-3})$ are called higher-order ionospheric (HOI) corrections.
As the GPS satellites emit microwave signals at two frequencies ($f_1 = 1575.42\,\text{MHz}$ and $f_2 = 1227.60\,\text{MHz}$), the first-order ionospheric refraction may be eliminated from the observation by forming the so–called ionosphere-free linear combination $L_{\text{if}} = (f_1^2 L_1 - f_2^2 L_2)/(f_1^2 - f_2^2)$, where L_1 and L_2 are the original carrier phase observations on the two frequencies (the same linear combination is used for code observations).
The HOI terms in Eq. (1) are not eliminated by forming the ionosphere-free linear combination. Their modeling requires the knowledge of the electron density and the magnetic field along the ray path (Hoque et al., 2008). All orbit and gravity field solutions presented here were obtained by using only the ionosphere-free linear combination. In Jäggi et al. (2015a) some attempts were made to mitigate ionosphere-induced problems in GOCE POD by means of HOI modeling, but the success was marginal.

Figure 2 (left) shows Swarm-A carrier phase residuals of two days with comparable orbit-Sun geometry (day 15/111: local time of ascending arc $\sim 17\,\text{h}$, day 15/233: local time of descending arc $\sim 18\,\text{h}$), but with substantially different mean TEC in die Earth's ionosphere, see Figure 2 (right). Note that the ionospheric disturbances are usually largest for the evening hours local time.

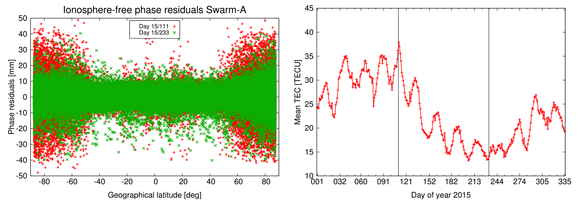

Figure 2: Left: carrier phase residuals of reduced-dynamic Swarm-A POD for days 15/111 (21-Apr-2015) and 15/233 (21-Aug-2015). Right: daily mean TEC as derived by the Center for Orbit Determination in Europe (CODE). The two vertical lines mark the days 15/111 and 15/233. $1\,\text{TECU} \equiv 10^{16}$ electrons/m^2.

Polar regions

The dynamics of the ionosphere can be directly derived from the GPS data by forming the so-called geometry-free linear combination $L_{\text{gf}} = L_1 - L_2$, which does not contain geometrical or clock information and, up to a carrier phase ambiguity, corresponds to the ionospheric refraction. Figure 3 (left) shows the time derivative dL_{gf}/dt computed from the observations of the Swarm-A receiver to one GPS satellite (G05) during 15.6 minutes when Swarm-A was at high latitudes ϕ (from $-60.0°$ to $-87.4°$ back to $-60.0°$).

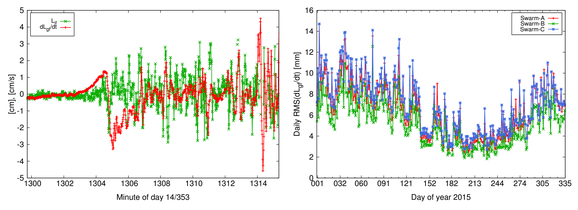

Figure 3: Left: time derivative of geometry-free linear combination L_{gf} (red, characterizing rate of change of ionospheric refraction) and ionosphere-free carrier phase residuals (green) for Swarm-A passing the south pole on day 14/353 (19-Dec-2014). Right: daily RMS of dL_{gf}/dt over all GPS satellites for polar passes ($|\phi| > 60°$).

From minute 1304 ($\phi = -76.2°$) onwards the ionospheric refraction shows massive high-frequency variations, resulting in a higher noise also in the L_{if} phase residuals. They are most probably scintillation. Such passes are very common for GPS observations gathered by spaceborne receivers at high latitudes. Often ionospheric refraction variations are so severe that the L_{if} observations to some GPS satellites are left out in the data preprocessing. Figure 3 (right) shows the daily RMS values of dL_{gf}/dt for all Swarm satellites and for polar passes. Note the clear correlation with the daily mean TEC in Figure 2 (right).

Equatorial regions

While scintillation-like behaviours of dL_{gf}/dt do occur also at low latitudes, the more important phenomena are slower variations of dL_{gf}/dt with larger amplitudes. This is illustrated in Figure 4.

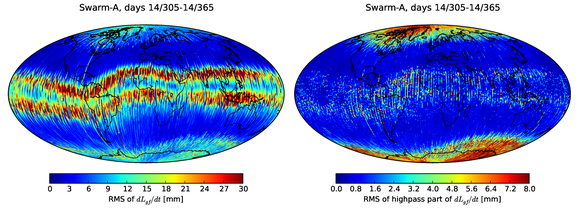

Figure 4: Geographically binned RMS of dL_{gf}/dt for Swarm-A. Left: the full signal dL_{gf}/dt is shown. Right: only the highpass part of dL_{gf}/dt is shown (a Gauss filter of width 100 s was used to filter each pass), indicating the geographical locations of scintillation-like features. The latter also appear for equatorial crossings, but the large RMS for low latitudes in the left plot is mainly due to the deterministic behavior shown in Figure 5 (left).

Figure 5 (left) shows an equatorial pass (from $30°$ to $-30°$ geographical latitude) for Swarm-A on November 1, 2014. Apart from dL_{gf}/dt (red) and the L_{if} residuals (green), the number of GPS satellites used for the kinematic positioning (blue) and the difference between the reduced-dynamic and the kinematic orbit in radial direction (magenta) are shown, as well.

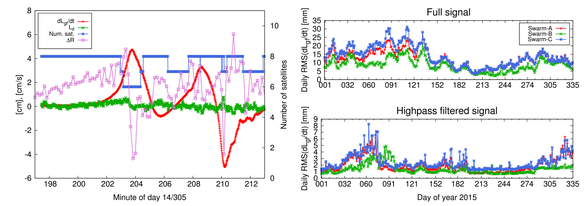

Figure 5: Left: Swarm-A passing the equator on day 14/305 (01-Nov-2014) west of South America. Red: time derivative of geometry-free linear combination L_{gf} (w.r.t. G04). Green: ionosphere-free carrier phase residuals. Blue: number of GPS satellites used for kinematic positioning. Magenta: difference between reduced-dynamic and kinematic Swarm-A orbit in radial direction. Right: daily RMS of dL_{gf}/dt over all GPS satellites for equatorial passes ($|\phi| < 30°$). The top figure shows the full signal, the bottom plot only the highpass part.

On minutes 204 ($\phi = 4.9°$) and 210 ($\phi = -18.1°$) the latter difference shows short deviations of several centimeters. Due to the stiffness of the reduced-dynamic orbit (6 minutes piecewise constant empirical accelerations were set up) these deviations have to be attributed to the kinematic orbit. The deviations coincide with large higher derivatives of L_{gf} and a drop of the number of satellites used for the kinematic positioning. The exact cause for these systematic shifts remains to be clarified. They might be related to the missing HOI corrections or to receiver-specific tracking problems. It is, on the other hand, clear that these deviations will be mapped into a gravity field solution recovered from these kinematic positions.

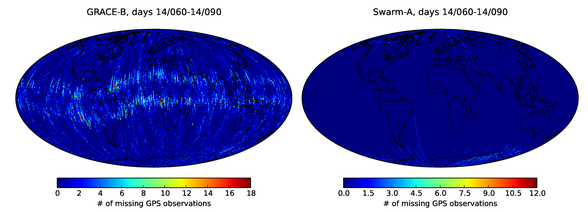

Figure 6: Number of missing GPS observations for GRACE-B (left) and Swarm-A (right) for March 2014. For these days the ascending arcs of GRACE-B and the descending arcs of Swarm-A passed the equator in the evening hours and the TEC was relatively high (38-44 TECU). While the Swarm receiver shows virtually no missing observations, the GRACE receiver skips a significant number of observations along the geomagnetic equator. Consequently, GPS-only GRACE gravity fields show no, or at least very much reduced spurious signals along the geomagnetic equator.

Impact of tracking loop settings

For the Swarm-A/-B/-C receiver the bandwidth of the L_1 carrier loop was increased by 50 % and the bandwidth of the L_2 carrier loop by 100 % on 08-Oct-2015 (day 281)/10-Oct-2015 (day 283)/06-May-2015 (day 126). Figure 7 shows the L_{if} carrier phase residuals separately for polar and equatorial passes. The modified bandwidths yield slightly reduced carrier phase residuals over the poles, but not over the equator. The increase of the Swarm-A and -B residuals on 06-May-2015 is due to an enlargement of the field of view without an update of the antenna phase center variations.

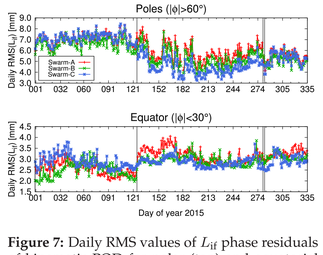

Figure 7: Daily RMS values of L_{if} phase residuals of kinematic POD for polar (top) and equatorial (bottom) passes. The three vertical lines indicate the days on which the tracking loop updates occurred.

Screening

A crude, but proven method for the mitigation of ionosphere-induced problems of orbits and gravity fields consists of skipping GPS data with dL_{gf}/dt exceeding a certain threshold. While for GOCE a suitable threshold was $5\,\text{cm/s}$, a more stringent value of $2\,\text{cm/s}$ is needed for Swarm (Jäggi et al., 2015b).

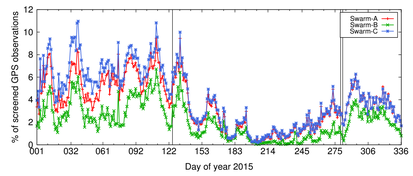

Figure 8: Percentage of Swarm GPS data with $dL_{\text{gf}}/dt > 2\,\text{cm/s}$. When omitting this data, the spurious signatures along the geomagnetic equator can be significantly reduced (see Figure 9). The three vertical lines mark the days on which the tracking loop updates occurred.

Figure 9 shows the impact of the GPS data screening on the Swarm gravity field.

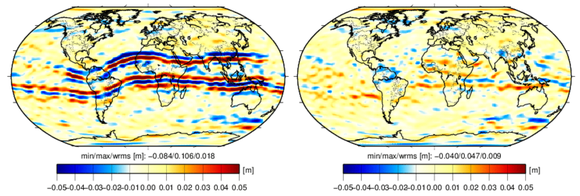

Figure 9: Bi-monthly combined Swarm gravity field (Nov and Dec 2014), recovered from kinematic orbits based on original (left) and screened (right) GPS data. The figures show the geoid height differences of degree and order 90 solutions w.r.t. GOCO05S, a 400 km Gauss filter was applied.

Conclusions

- Ionospheric disturbances have an important effect on GPS-based LEO POD and gravity field recovery, even when using the ionosphere-free linear combination.
- The first time derivative of the geometry-free linear combination L_{gf} is used to characterize the behavior of the ionospheric refraction. For Swarm, scintillation-like features of dL_{gf}/dt occur mainly at high latitudes, while the equatorial crossings are characterized by large, but deterministic changes of dL_{gf}/dt.
- The variations of the ionospheric refraction over the equator induce systematic biases in the kinematic positions. They map into gravity fields recovered from these positions. While unconsidered HOI modeling might play a role, receiver-specific tracking problems might be responsible, as well. In such a case, the GPS data gathered around the geomagnetic equator is systematically distorted and its use (not only for orbit and gravity field determination) must be questioned.

References

Hoque, M. M., and Jakowski, N. (2008) Estimate of higher order ionospheric errors in GNSS positioning. Radio Sci., 43, RS5008, doi:10.1029/2007RS003817

Jäggi, A., Bock, H., Meyer, U., Beutler, G., van den IJssel, J. (2015a) GOCE: assessment of GPS-only gravity field determination. J Geod 89:33-48, doi:10.1007/s00190-014-0759-z

Jäggi, A., Dahle, C., Arnold, D., Bock, H., Meyer, U., Beutler, G., van den IJssel, J. (2015b) Swarm kinematic orbits and gravity fields from 18 months of GPS data. Adv Space Res, in press, doi:10.1016/j.asr.2015.10.035

Contact address

Daniel Arnold
Astronomical Institute, University of Bern
Sidlerstrasse 5
3012 Bern (Switzerland)
daniel.arnold@aiub.unibe.ch

Poster compiled by Daniel Arnold, December 2015
Astronomical Institute, University of Bern, Bern
daniel.arnold@aiub.unibe.ch